Comptes Rendus

Chimie

Jemaa Mabrouki, Mohammed Ammar Abbassi, Besma Khiari, Salah Jellali and Mejdi Jeguirim

Investigations on potential Tunisian biomasses energetic valorization: thermogravimetric characterization and kinetic degradation analysis

Part of Special Issue: Sustainable Biomass Resources for Environmental, Agronomic, Biomaterials and Energy Applications 3

Guest editors: Mejdi Jeguirim (Université de Haute-Alsace, Institut de Sciences des Matériaux de Mulhouse, France), Salah Jellali (Sultan Qaboos University, Oman) and Besma Khiari (Centre of Water Researches and Technologies, Tunisia)

Sustainable Biomass Resources for Environmental, Agronomic, Biomaterials and Energy Applications 3 / *Ressources de biomasse durables pour des applications environnementales, agronomiques, de biomatériaux et énergétiques 3*

Investigations on potential Tunisian biomasses energetic valorization: thermogravimetric characterization and kinetic degradation analysis

Jemaa Mabrouki [a]**, Mohammed Ammar Abbassi** [a]**, Besma Khiari** [*, b]**, Salah Jellali** [c]
and Mejdi Jeguirim [d]

[a] Unité de Recherche Matériaux, Energie et Energies Renouvelables (MEER), Faculté des Sciences de Gafsa, B.P.19, Zarroug, Gafsa, 2112, Tunisia

[b] Wastewaters and Environment Laboratory, Water Research and Technologies Center (CERTE), Technopark Borj Cedria, University of Carthage, P.O. Box 273, Soliman 8020, Tunisia

[c] Center for Environmental Studies and Research, Sultan Qaboos University, Al-Khoud 123, Muscat, Oman

[d] The institute of Materials Science of Mulhouse (IS2M), University of Haute Alsace, University of Strasbourg, CNRS, UMR 7361, F-68100 Mulhouse, France

E-mails: jemaa_mabrouki@hotmail.com (J. Mabrouki), abbassima@gmail.com (M. A. Abbassi), besmakhiari@yahoo.com (B. Khiari), s.jelali@squ.edu.om (S. Jellali), mejdi.jeguirim@uha.fr (M. Jeguirim)

Abstract. In this work, six Tunisian local biomasses, namely ziziphus wood (ZW), almond shells (AS), olive stones (OS), vine stems (VS) and date palm leaflets (DPL) and trunks (DPT) were slowly pyrolyzed under inert atmosphere at a heating rate of 5 °C/min through thermogravimetric (TG) analyses. The thermal degradation of samples involves the interaction in a porous media of heat, mass and momentum transfer with chemical reactions. Heat is transported by conduction, convection and radiation and, mass transfer is driven by pressure and concentration gradients. Thermal degradation curves have been studied with minute details for each degradation step. The Coats–Redfern model was used to extract the kinetic parameters from the TG data, then the kinetic parameters such as the activation energy, the pre-exponential factor and the order of the reaction were calculated. Results showed that the total mass losses amounts and kinetics are dependent on the type of the used biomass. Moreover, the devolatilization could be described by the first order model, while the char formation stage was better described by the second and third order reactions model. The physico-chemical characteristics of these samples were also determined. The volatile matter (VM) content varies considerably, with values ranging from 67.19% for AS to 77.4% for ZW. The maximum values were obtained for ZW and VS with values of 77.4% and 71.9%, respectively. The lowest value (67.19%) was determined for AS. In addition, the ash contents vary between 0.8% for OS and 5.66% for DPT.

* Corresponding author.

The ashes vary significantly from one sample to another, with the values being even lower than 1% for OS, whereas the higher values in the DPT is 5.66%. Further, activation energies corresponding to main devolatilization regions were 59.5, 47.0, 55.8, 41.1, 89.1, 45.2 kJ/mol for ZW, AS, OS, VS, DPL, and DPT respectively. Among all the tested biomasses, the ZW and VS appear to have an important potential to be used for energy production.

1. Introduction

The utilization of renewable resources derived from plant biomasses for energetic purposes will reduce the reliance on the limited fossil fuels and has various positive environmental impacts such as the reduction of greenhouse gas emissions and the preservation of water resources against pollution [1]. Biomasses have been considered as the oldest source of energy since several millennia. Nowadays, biomasses represent about 14% of the overall available world's primary energy reserves and its use accounts for 3% and 35% for developed and developing countries, respectively [2]. Energy recovery from biomasses is currently considered as an attractive and sustainable management option as long as there is no overexploitation of these resources [3]. In addition, the use of biomasses as an energy source participates in the natural carbon cycle. Indeed, the quantity of carbon dioxide released during the thermal treatment of biomasses corresponds substantially to that absorbed by photosynthesis during plants growth. Basically, thermogravimetric analysis (TGA) is an analytic method that allows the following of the mass loss of a given sample versus temperature or time. The application of this technique for biomasses has also various applications such as the determination of their thermal stability, the impurities, the hydration rate, and the volatile matter, the fixed carbon and the ash contents [4]. It is also the adapted tool for calculating the main kinetic parameters such as the activation energy, the involved reaction order and the frequency factor [5,6]. The thermogravimetric analysis was applied and discussed for various biomasses [7–9]. The use of kinetic models for the interpretation of the thermal degradation of biomasses experimental data could be very helpful for the optimization of the overall pyrolysis process [10]. For instance, Gasporovic *et al.* studied the thermal degradation of wood wastes. They found that this operation occurs in three stages corresponding to water evaporation, an active, and a passive degradation phase, respectively [11]. Moreover, Gronli *et al.* investigated the thermal decomposition of two types of wood (hardwoods and softwoods) [12]. Comparison between these samples thermal behavior shows that the degradation of softwood starts at lower times and the hemicellulose and cellulose decomposition zones are wider than the hardwood biomass. Besides, Slopiecka *et al.* examined the kinetic degradation of a poplar wood, using three different models, namely Kissinger, Kissingere–Akahirae–Sunose (KAS) and Flynne–Walle–Ozawa (FWO) methods [13]. The results showed that both FWO and KAS models fitted well the experimental date and were suitable for the assessment of the involved mechanisms during the degradation of the used lignocellulosic materials. Thermogravimetric analysis is the most common technique used to estimate the kinetic triplets and thermodynamic parameters of pyrolysis process [14,15]. In addition, Jeguirim *et al.* investigated the thermal degradation behavior of five tropical biomasses using thermogravimetric method [16]. Their research highlighted the importance of a better understanding of the involved mechanisms in the thermal degradation for the optimization of energy production. This is a very important step for the pyrolysis process design, expediency, assessment and scaling up for industrial processes. It is however very important to underline that the involved mechanisms during the pyrolysis of biomasses is still misunderstood due mainly to the little real progress made on the precise quantification of the chemical reactions on the solid matrix [17]. In Tunisia, various agricultural residues and agro-industrial byproducts are produced in relatively important amounts all over the year. Among these wastes, zizyphus wood, almond shell, olive residues, vine stems and date palm residues are abundant lignocellulosic biomass resources in Tunisia [18]. The sustainable management of these wastes has been stressed by the national concerned stakeholders

since several decades ago. The thermochemical conversion of these biomasses for energy and resources recovery has been pointed out as technically feasible, economically attractive and environmentally friendly option [19–22]. For instance, in 2017, the produced olive mill solid wastes in Tunisia were evaluated to 0.450 million tonnes. Different valorization options have been studied at small laboratory scale. They included their combined treatment through adsorption onto sawdust and electrocoagulation [23], their thermal conversion through pyrolysis into biofuels and biochars for energetic, environmental and agronomic purposes [7,24] as well as their thermochemical modification for the generation of activated carbons for efficient industrial effluent treatment [25–27]. The use of kinetic models for fitting the experimental data obtained during the pyrolysis of these wastes is a very important. The thermal kinetics of date palm residues samples can be examined under non-isothermal conditions at various different heating rates [18]. The calculation of these parameters are usually based on the Arrhenius equation and, the linear regression method is often used [4,9,28]. However, to the best of our knowledge, this task has not been carried out for the ziziphus wood. The main aim of the current work is to assess the devolatilization kinetic parameters characterizing six Tunisian biomasses: ziziphus wood, almond shell, olive stones, vine stems and date palm leaflets and trunks by using the experimental data from non-isothermal TG and the Coats and Redfern calculation method. In addition, a comparison of these thermal characteristics was carried out in order to determine their ability for bioenergy production.

2. Materials and methods

2.1. *Biomasses preparation, characterization and TG analysis procedure*

The six used biomasses (Figure 1) were collected form the region of Gafsa (south of Tunisia). They were firstly air-dried under sunlight for a period of 7 days. Then, they were manually crushed and grounded in order to obtain homogenous samples. The retained fraction during this work has particle dimensions lower than 1 mm. Elementary composition was investigated with a CHNS-O Analyzer model 2400. The proximate analysis was based on the thermogravimetric analysis (TGA) results carried out by using the ATG/ATD Setaram Setsys Evaluation instrument. Inherent moisture content is determined by heating an air-dried sample at 105 °C–110 °C under specified conditions until a constant weight is obtained. Volatile matter is defined as the gases removed when the sample is heated to 950 °C under inert atmosphere. The ash content is the amount left when oxygen is injected at 950 °C after volatiles removal. Fixed carbon is obtained by difference.

The thermal degradation behavior of the differents samples were performed using TG analysis. During these analyses, 10 mg of each sample was heated up to a final temperature of 800 °C for a fixed heating gradient of 5 °C/min. These assays were carried out by using nitrogen as an inert gas at a flow rate of 12 NL/h. The used parameters, final temperature reactions of 800 °C, 10 mg of each sample, and the heating rate of 5 °C/min are chosen when doing TGA-experiments for kinetic studies which are considered one important task to decide the heating rate with an appropriate sample size [6]. The optimal condition, which causes minimal heat and mass transfer problems, can be obtained by using very low heating rates and very small sample size. The determination of kinetic mechanisms is mainly carried out under regimes controlled by chemical kinetics, by using very small samples in powder form so that effects of transport phenomena such as heat and mass transfer can be neglected [29–31].

2.2. *Thermal degradation kinetics assessment*

The obtained experimental data (TG and DTG) curves for all the six followed biomasses were used to determine the corresponding kinetic parameters in a first step and then to deduce the most probable involved degradation mechanisms.

The biomass degradation kinetic model is typically given by the Arrhenius equation as follows:

$$\frac{\mathrm{d}\alpha}{\mathrm{d}t} = k(T)f(\alpha) \tag{1}$$

where α represents the degree of degradation of the biomass, $f(\alpha)$ is a function depending on the involved decomposition mechanism, $k(T)$ is the decomposition rate function, T is the temperature and t the time.
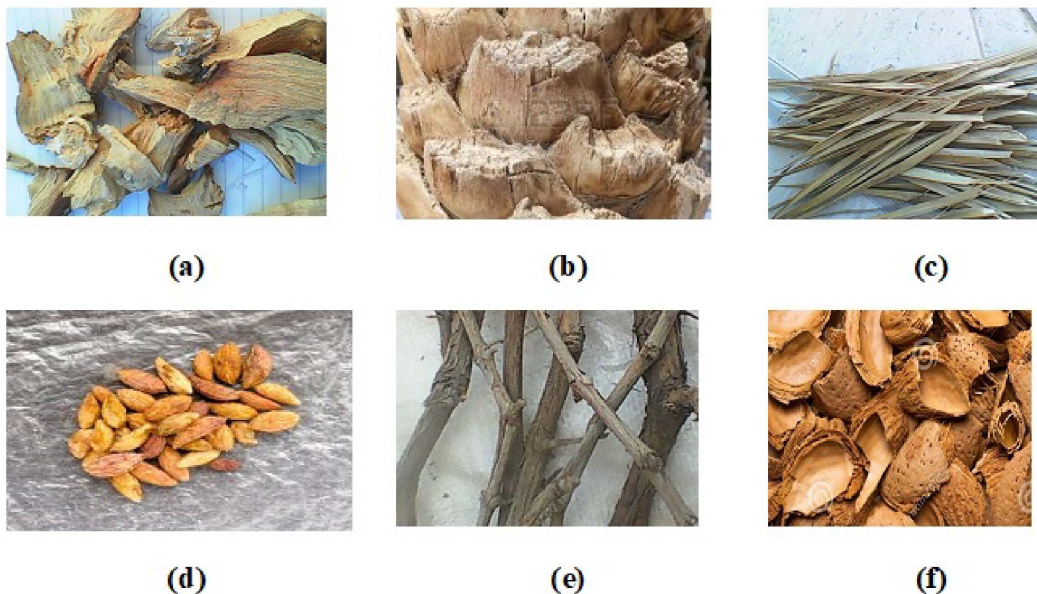
Figure 1. Lignocellulosic materials: (a) ziziphus wood, (b) date palm trunk (c) date palm leaflets, (d) olive stone, (e) vine stems, (f) almond shell.

The α parameter can be calculated for the TG curves as below:

$$\alpha = \frac{m_i - m_t}{m_i - m_f} \qquad (2)$$

where m_i, m_t and m_f are the initial biomass mass, at a given time t and at the end of the analysis, respectively.

The function $f(\alpha)$ depends on the order of the reaction "n" as follows:

$$f(\alpha) = (1 - \alpha)^n. \qquad (3)$$

The constant rate $k(T)$ is given by the Arrhenius equation:

$$k_i = k_{0i} \left(\frac{-E_{ai}}{RT} \right) \qquad (4)$$

where k_{0i} is the pre-exponential factor (time^{-1}), E_{ai} is the activation energy (kJ·mol^{-1}), T is the temperature (°C) and R is the universal gas constant (J·K^{-1}·mol^{-1}).

In the case of a constant heating rate (β): $\beta = dT/dt = cste$, the variation of degree of decomposition can be written as a function of temperature as follows:

$$\frac{d\alpha}{dT} = \frac{A}{\beta} \exp \left(-\frac{E}{RT} \right) f(\alpha) \qquad (5)$$

where A is the Arrhenius—pre-exponential factor.

$$\frac{d\alpha}{f(\alpha)} = \frac{A}{\beta} \exp \left(-\frac{E}{RT} \right) dT. \qquad (6)$$

The integration of (6) gives:

$$g(\alpha) = \int_0^\alpha \frac{d\alpha}{f(\alpha)} = \frac{A}{\beta} \int_0^T \exp \left(-\frac{E}{RT} \right) dT. \qquad (7)$$

The right hand side of (7) has no exact analytical solution. However, its resolution can be carried out by the asymptotic approximation according to the Coats and Redfern method. When neglecting the high order terms of this solution, the (7) can be transformed as follows:

$$g(\alpha) = \frac{ART^2}{\beta E} \left(1 - \frac{2RT}{E} \right) \exp \left(-\frac{E}{RT} \right). \qquad (8)$$

Then, after division by T^2 and taking logarithms, Equation (8) becomes:

$$\text{Ln} \frac{g(\alpha)}{T^2} = \text{Ln} \frac{AR}{\beta E} \left(1 - \frac{2RT}{E} \right) - \frac{E}{RT}. \qquad (9)$$

Since $(2RT/E \ll 1)$, the (9) can be transformed in:

$$\text{Ln} \frac{g(\alpha)}{T^2} = \text{Ln} \frac{AR}{\beta E} - \frac{E}{RT}. \qquad (10)$$

The plots giving $\ln[g(\alpha)/T^2]$ versus $1/T$ give access to the E parameter through the calculus of the corresponding slope. The term $\text{Ln}(AR/\beta E)$ is nearly

Table 1. Algebraic expressions of functions used for biomass thermal degradation

Kinetic model	$f(\alpha)$	$g(\alpha) = \int_0^\alpha \dfrac{\mathrm{d}\alpha}{f(\alpha)}$	Symbol
First order	$1 - \alpha$	$-\ln(1 - \alpha)$	F1
Second order	$(1 - \alpha)^2$	$[1/(1 - \alpha)] - 1$	F2
Third order	$(1 - \alpha)^3$	$(1/2)([1/(1 - \alpha)^2] - 1)$	F3

constant and its calculus permits the assessment of the Arrhenius—pre-exponential factor A [18]. The expressions of the functions $f(\alpha)$ and $g(\alpha)$ depend on the conversion mechanism and its corresponding mathematical models. Table 1 gives the kinetic models used in the current study for deducing, from the TG curves, the most probable mechanisms during the pyrolysis of the six studied biomasses. Three chemical reaction models were used, namely the first-order (F_1), the second order (F_2) and the third order (F_3) models.

3. Results and discussion

3.1. *Biomasses characterization*

The ultimate and proximate analysis for the six studied biomasses were carried out according to the experimental protocols given in Section 2.1 and the corresponding results are given in Tables 2 and 3 and compared with some reults of literature [33]. Table 2 gives the elementary analysis as well as the "H/C" and "O/C" ratios of the ziziphus wood (ZW), almond shell (AS), olive stones (OS), vine stems (VS) and date palm leaflets (DPL) and trunks (DPT) which are 0.13, 0.14, 0.10, NC, 0.13, 0.13 and 0.79, 1.06, 0.86, 1.03, 0.79, 0.82 respectively. All samples have an elementary composition close to the classical value for lignocellulosic biomass [34]. From Table 2, it can be seen that all the studied biomasses have relatively high C and O contents. The maximum C contents were observed for olive stones followed by vine stems with respective values of about 52.9% and 48.2%, respectively. This might be attributed to the high lignin percentage in OS and VS. Actually, the lowest C contents were observed for DPL and DPT with values of about 46.2% and 43.7%, respectively. The O contents varied between about 36.2% and 49.9% for DPT and VS, respectively. Similar results were reported by Slopiecka *et al.* for Poplar wood [13]; the elements of

carbon (C), hydrogen (H), nitrogen (N) and oxygen (O) were 45.5%, 6.26%, 1.04% and 47.2%, respectively. According to Pala *et al.*, apple pomace also have the greatest elemental amount of carbon (47.98%) and oxygen (37.44%) [35]. In addition Kim *et al.* also reported similar results for Pinyon pine wood. Carbon, hydrogen, nitrogen and oxygen O were 41.92%, 6.0%, 2.97% and 49.11%, respectively [36]. Present results revealed O/C ratios ranging from 0.79 to 1.06. The comparison of the different samples shows that ZW, DPL have the lowest O/C ratio while the highest O/C ratios are for AS and VS. Furthermore, the S contents were low for AS and ZW (Table 2) indicating that the SO_x gas emissions during the pyrolysis of these biomasses would be low for these two biomasses as previously reported by Grioui *et al.* for the Tunisian olive wood [37]. In general, N and S contents are low (around 1% or lower). Yet, small amounts of N and S might be advantageous because they could minimize the corrosion problems associated with the formation of acids in the process equipment [38]. Unfortunately, N and S contents were high for the two date palm biomasses and therefore the related emissions of NO_x and SO_x could result in corrosion problems. These results are consistent with previous reports in the scientific literature [39]. On the other hand, the proximate analysis results showed that, for all the studied biomasses, volatile matter (VM) contents are quite high (Table 3). Volatiles vary considerably, with values ranging from 67.19% for AS to 77.4% for ZW. The VM correspond mainly to the cellulose and hemicellulose that will be degraded during the pyrolysis process for the formation of biofuels (biogas and bio-oil). This composition makes, therefore, AS and ZW attractive materials for bioenergy production. Similar results concerning for example the grape pomace biomass were reported [40]. In addition, the ash contents vary between 0.8% for OS and 5.7% for DPT. These values are in the range of reported values in the literature [41–43]. The fixed

Table 2. Ultimate analyses of the used biomasses

Biomass	Carbon	Hydrogen	Oxygen	Nitrogen	Sulfur	H/C ratio	O/C ratio	
ZW	46.21 ± 0.85	5.78 ± 0.09	36.54 ± 1.44	0.51 ± 0.02	$0.021 \pm 9 \times 10^{-4}$	$0.13 \pm 4 \times 10^{-3}$	0.79 ± 0.02	
AS	46.86 ± 0.92	6.19 ± 0.10	49.75 ± 1.24	<0.5	<0.05	$0.14 \pm 4 \times 10^{-3}$	1.06 ± 0.037	
OS	52.89 ± 1.31	5.28 ± 0.11	45.85 ± 1.65	ND	ND	$0.10 \pm 3 \times 10^{-3}$	0.86 ± 0.01	This work
VS	48.16 ± 1.46	ND	49.85 ± 1.34	ND	ND	NC	1.03 ± 0.04	
DPL	46.16 ± 1.76	5.84 ± 0.14	36.54 ± 1.41	2.15 ± 0.08	0.39 ± 0.01	$0.13 \pm 5 \times 10^{-3}$	0.79 ± 0.01	
DPT	43.74 ± 1.11	5.66 ± 0.12	36.20 ± 1.66	0.69 ± 0.02	0.35 ± 0.01	$0.13 \pm 4 \times 10^{-3}$	0.82 ± 0.02	
Cassava pulp residue	35.89	5.47	58.27	0.36	ND	1.829	1.218	[32]
Palm kernel cake	47.19	6.38	43.28	3.15	ND	1.622	0.688	[32]
Longan fruit seed	43.75	6.30	48.81	1.14	ND	1.350	0.668	[32]
Coconut shell	49.76	5.60	44.30	0.35	ND	1.727	0.837	[32]

Table 3. Proximate analyses of the used biomasses

Biomass type	Moisture	FC	VM	Ash	HHV (MJ/kg)	
DPT	7.32 ± 0.34	17.26 ± 0.67	69.76 ± 2.11	5.66 ± 0.02	17.68 ± 0.72	
AS	7.07 ± 0.52	22.3 ± 0.92	67.19 ± 1.96	3.45 ± 0.01	19.76 ± 1.13	
VS	6.45 ± 0.29	19.94 ± 0.88	71.9 ± 2.32	1.71 ± 0.03	NC	This work
ZW	5.75 ± 0.12	15.44 ± 0.54	77.44 ± 3.12	1.37 ± 0.01	18.50 ± 0.54	
DPL	6.75 ± 0.29	17.67 ± 0.76	70.21 ± 3.11	5.37 ± 0.04	18.52 ± 0.79	
OS	9.19 ± 0.04	22.68 ± 1.08	67.33 ± 2.09	$0.80 \pm 2 \times 10^{-3}$	20.84 ± 0.32	
Cassava pulp residue	ND	11.83	81.98	6.19	22.41	
Palm kernel cake	ND	16.74	79.57	3.69	21.91	[33]
Longan fruit seed	ND	14.80	84.51	0.70	21.16	
Coconut shell	ND	16.33	82.38	1.29	21.28	

carbon values of the studied biomasses vary between 15.4% and 22.7% for ZW and OS, respectively. This is typical for biomass types derived from hard tissues such as trunks, while in case of soft tissues (such as leaves, young branches, bushes, grasses, etc.), the content is as low as 17.67% for DPL. Moreover, the low ashes (1.37%) and the high volatiles (77.44%) for ziziphus wood, are characteristic of lignocellulosic materials, which make this biomass very attractive for the thermal degradation processes. The vegetable biomass samples coming from different plant types or even from different parts of the same plant have significantly different fixed carbon and ash contents [44,45]. The higher ash content associated with AS, DPL and DPT would likely make lignin difficult to decompose during the pyrolysis; the generated solid residue would be very high. The mineral composition of the followed biomasses is given in Table 4. The presence of K, Na and Ca elements in biomasses with important contents could negatively impact their thermal degradation and therefore promote the formation of biochars. Moreover, the calculus of the sum of the main contents (P and Mg) is particularly important to highlight if the generated biochars could be valorized as biofertilizers in agriculture. To sum up, it is interesting to note that the low moisture and ash content and high volatile make ziziphus wood and vine stems two potential sources for energy generation and/or bio-chemicals production in Tunisia. Finally, for the feedstock producing higher amounts of ash during pyrolysis, ash removal systems should be envisaged when designing the conversion process. composition of biomasses is volatile contents and carbon and oxygen are the major elements. The gross heating values of all biomasses varied approximately from 17.68 to 20.84 MJ/kg. According to Damartzis *et al.* who studied the Tthermal degrada-
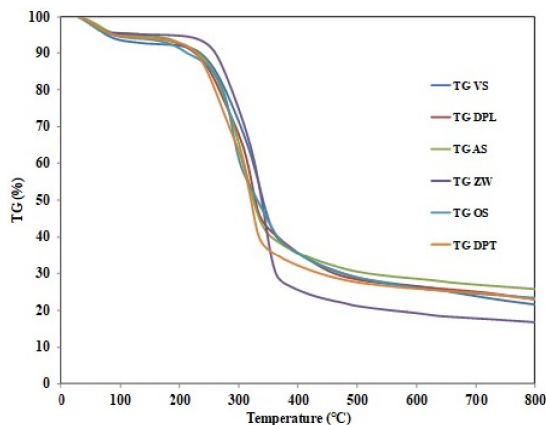
Figure 2. TGA curves of the different samples under nitrogen atmosphere.
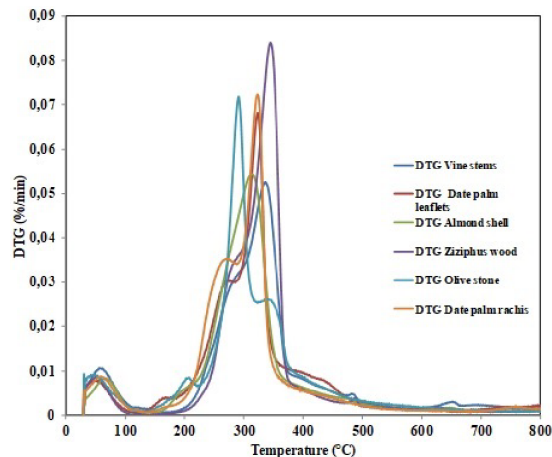

Figure 3. DGA curves of the different samples under nitrogen atmosphere.

tion and kinetic modeling of cardoon (Cynara cardunculus) pyrolysis using thermogravimetric analysis (TGA), the highest calorific value corresponded to stems (21.5 MJ/kg), due to their lower ash and higher volatiles content while the HHV value of Cardoon leaves was 17.9 MJ/kg. The stems are lower in inorganic constituents than the leaves (ash content 7.6%) [46]. In fact, even if the main goal of this study is to identify the biomass that is considered the most energetic for the production of three components: bio-oil, gas, and char, the yielded char characteristics are so interesting that it may be used in different applications, such as the production of chemicals, activated carbon, carbon nanotubes, carbon fibers, etc. The produced char is also a better fuel than the precursor biomass, which means that it can be used as a high-efficiency solid fuel (converted into briquettes alone or mixed with biomass) in boilers.

3.2. *Thermal analysis*

The thermal analysis of the six studied biomasses was carried out under the experimental conditions given in Section 2.2. The corresponding TGA and DTG profiles were given in Figures 2 and 3, respectively. For all the followed biomasses, the curves revealed the presence of three identical degradation zones corresponding to the moisture evaporation, the decomposition of the volatile matter and the production of the solid residue, in agreement with previous findings [47,48]. The deshydratation zone is

observed at temperature values between room temperature and 105 °C, 108 °C, 90 °C, 145 °C, 90 °C and 110 °C respectively for ZW, AS, OS, VS, DPL and DPT. During this phase, the mass loss is negligible attributed to the removal of moisture and the start of polysaccharide hydrolysis [49,50]. The second stage of mass loss depicted in Figures 2 and 3 ranged from 145 °C to 400 °C and corresponds mainly to the degradation of hemicelluloses, cellulose and lignin. Hemicelluloses typically decomposes between 160 and 360 °C, while cellulose degrades at higher interval of 240–390 °C. The third stage of decomposition (from 400 to 900 °C) is attributed to lignin. The degradation of lignin typically happens at a slow rate over a much wide temperature range of 180–900 °C [51]. Such variations in the lignin starting degradation temperatures of the six biomasses could be linked to the differences in their elemental and chemical compositions. The maximum weight loss occurs in the range 200–400 °C. During this period, the hemicelluloses and cellulose were degraded and, volatiles, gases, and primary bio-char are produced [52]. According to Miranda *et al.,* this stage of biomass decomposition corresponds to the beginning of secondary decomposition of heavier volatiles and the formation of char [53]. Furthermore, a similar behavior was observed by Ceylan *et al.* during the pyrolysis of hazelnut shells at 5 °C/min [54]. The authors assumed that the decomposition of a part of the biomass (hemicellulose and cellulose) occurs in two ways. In the

Table 4. Mineral composition of the studied biomasses (%)

Element	ZW	AS	OS	VS	DPL	DPT
Na	0.216	0.089	–	0.319	0.100	0.102
Mg	0.080	0.084	0.115	0.198	0.281	0.575
Al	0.023	0.050	0.008	0.042	0.024	0.011
Si	0.081	0.146	0.058	0.096	0.223	0.187
P	0.058	0.089	0.110	0.019	0.261	0.148
Cl	0.070	0.038	0.132	0.273	1.858	2.847
K	0.063	0.956	0.435	0.176	2.544	2.485
Ca	0.779	0.732	0.085	0.645	0.494	0.492
Fe	0.063	0.061	0.103	0.050	0.035	0.026
Cu	0.029	0.018	0.019	0.015	0.041	0.040
Zn	0.322	0.047	0.091	0.070	0.021	0.035
Sr	0.011	0.013	–	0.017	0.04	0.005

first mode, which occurs at low temperature (up to 355 °C in their study), the boundaries of the polymers decompose and generate CO and CO_2 gases as well as the carbon residue. In the second way, which occurs at high temperatures, leads to the formation of a liquid. In the third stage, the mass loss of the ZW, VS, OS, AS, DPL and DPT was less than that obtained in the second stage. The authors also showed that lignin is the main compound responsible for the production of char. The percentage of this carbonaceous residue is in the range 45–50% of the initial mass. The same percentage of char (40%) was found by Yang *et al.* in a wider temperature range (160–900 °C) [55]. These authors stated that in terms of energy consumption during pyrolysis, the behavior of cellulose differs from hemicellulose and lignin. During the first decomposition zone, the DTG curves of all biomasses show two distinct peaks (Table 5).

On the DTG profiles, the temperatures at which the maximum rate of mass loss occurred are described by the position of the peaks in the curve. The DTG peaks are much closer to each other for ZW than for OS and the maximum of hemicelluloses and cellulose peaks occurring at lower temperatures. Orfão *et al.* reported that the DTG peak during the decomposition of pure cellulose occurred at (332 °C, 0.9 wt%·s^{-1}) [56]. The second DTG peak, has a much higher rate of weight loss than the first stage. The thermal decomposition depends on the chemical composition of the biomasses as individual components of lignocellulosic materials have dif-

ferent thermal behaviors. Numerous studies on the thermal degradation of lignocellulosic materials indicated that the decomposition of hemicelluloses starts first, followed by the cellulose cracking and ends with the lignin degradation [57–59].

The comparison between the samples thermal behavior shows that the degradation of softwood starts at lower temperature and the hemicellulose and cellulose decomposition zones are wider than the hardwood biomass. It has been debated in the literature that the two different regions of weight loss observed for wood pyrolysis may be represented as a combination of the individual decomposition of hemicellulose and cellulose. The decomposition of parts of the biomass, due to pyrolysis, takes place in two ways because the kinetic model supposes that degradation reactions are beginning separately. First, hemicellulose and cellulose decompose and then lignin. For each decomposition reaction kinetic parameters are determined but they are only valid for a temperature domain.

The different chemical composition of wood, i.e. the different percentage of cellulose, hemicellulose and lignin, the different amount and composition of inorganic matter which leads to different starting degradation temperature.

This is consistent with the relatively simple chemical structure of cellulose, hemicellulose and lignin. However, some differences may be observed with respect to: (1) the width of the DTG peaks; (2) the temperature where the maximum rate of decomposition

Table 5. Peaks of pyrolysis DTG

Biomass	First peak		Second peak	
	Temperature (°C)	Mass loss rate (%·s^{-1})	Temperature (°C)	Mass loss rate (%·s^{-1})
ZW	285	0.035	344	0.084
VS	287	0.031	330	0.053
AS	207	0.006	310	0.054
OS	205	0.031	290	0.071
DPL	270	0.031	326	0.067
DPT	269	0.035	320	0.071

occur (Tpeak); and (3) the final char yield among the different samples analyzed. The Ziziphunus wood has different behavior due to higher cellulose content comparing the other polymers. In fact, it is well known that in the pure cellulose decomposition peak temperature is around 360 °C in similar TGA conditions. Woody biomasses are known to have higher cellulose content. For the other biomasses, the content of hemicellulose and cellulose is quite similar. Therefore, the peak of decomposition occurs earlier at lower decomposition rate.

In contrast to cellulose, lignin shows a gradual loss of weight from about 200 °C to the final temperature of 500 °C consistent with the wide variety of functional groups and hence bond strengths exhibited in the structure of lignin. In order to prove this behavior, one can see the weight or percentage of char at the final temperature (approximately 50% of the original lignin substance), which means that the lignin part of wood is mainly responsible for the char portion of the products.

Other studies of xylan have indicated a much lower char yield for the hemicelluloses and that they are the least thermal stable major component of wood. This is probably due to their lack of crystallinity.

ZW and DPL have almost similar chemical composition, which is reflected by their almost similar thermal fingerprints. It has been shown in the literature that the two different regions of weight loss observed for wood pyrolysis may be represented as a combination of the individual decomposition of hemicellulose and cellulose.

3.3. *Kinetics parameters*

The kinetic parameters obtained during the pyrolysis of the six studied biomasses are presented in Table 6. Initial pyrolysis temperatures, the peaks position and height in TGA and DTG curves show the reactivity of these samples. Samples with the highest cellulose content have the highest activation energies. In deed, the energy activation value of cellulose is the highest one (between 100–200 kJ/mol). When cellulose is present in significant amount, the activation energies or the frequency factors are higher (case of Ziziphunus Wood). The calculated average activation energies are comparable to those met in literature [60,61]. For example, Parthasarathy *et al.* carried out a similar study on rice husk [62]. They reported an activation energy around 55 KJ/mol for the first reaction zone of dehydration, 84.1 KJ/mol for the second zone (hemicelluloses and cellulose cracking) and 21.2 KJ/mol for the third reaction zone (lignin degradation). The kinetic approach shows that the devolatilization step could be described by the first order chemical reaction model (F1) while the second and third reaction orders (F2, F3) could fit the char formation. Moreover, several investigations showed that F1 could be a reasonable mechanism for describing the devolatilization phase of the biomass species. A similar conclusion was reached by Gil *et al.* who noted also two devolatilization stages during their work on the thermal behavior of pine and pine/coal blends [63]. The chemical reaction F1 mechanism could not be selected as an effective mechanism for this type of tropical biomass. Finally, the activation energy values do agree reasonably well with those obtained for other agricultural and forestry residues while applying the Coat Redfern

Table 6. Kinetics parameters of the thermal degradation of the studied biomasses

Biomass	Temperature range	Activation energy (kJ·mol^{-1})	Frequency factor (s^{-1})	R^2	Function $f(\alpha)$
ZW	241–362	59.5	182.6	0.9908	F1
	362–612	17.9	0.092	0.9965	F2
	362–612	48.3	527.1	0.9979	F3
AS	228–362	47.0	17.64	0.9906	F1
	362–645	18.8	0.091	0.9968	F2
	362–645	50.3	505.3	0.9982	F3
OS	241–362	55.8	18.5	0.9908	F1
	362–612	17.7	0.088	0.9965	F2
	362–612	49.2	29.3	0.9979	F3
VS	228–378	41.1	3.233	0.9933	F1
	378–553	14.6	0.026	0.9924	F2
	378–553	38.4	26.90	0.9908	F3
DPL	241–362	89.1	4.78	0.9968	F1
	362–612	15.88	0.067	0.9908	F2
	362–612	58	505.9	0.9987	F3
DPT	241–362	45.2	3.88	0.9956	F1
	362–612	19.3	0.077	0.9906	F2
	362–612	45	405.3	0.9986	F3

method [5,32].

4. Conclusions

Thermal decomposition of six Tunisian biomasses was analyzed by the thermogravimetric technique, which helped (i) assessing the main thermal characteristics such as the degradation temperature corresponding to the loss of mass and (ii) calculating the kinetic constants (the activation energy and the pre-exponential factor). The kinetic approach showed that the devolatilization step could be fitted by the first reaction order model while the char formation is better described by the second and third reaction orders. The average activation energies ranged from 15 to 89.1 kJ/mol for the first decompistion, from 14.6 to 19.3 kJ/mol for the second one and, from 38.4 to 58 kJ/mol in the last one. Ziziphus wood (ZW), almond shell (AS), olive stones (OS), vine stems (VS), date palm leaflets (DPL) and date palm trunks (DPT) have low sulphur and ash contents. The high volatile matter contents, related to the oil contentment of the residues, make them interesting sources for thermal energy production, notably for ziziphus wood and vine stems, which appear to be more desirable feedstock for pyrolysis and upgrading applications compared to other samples. As for the feedstock that produce higher amounts of ash during pyrolysis, ash removal systems should be set up when designing the conversion process.

Conflicts of interest

Authors have no conflict of interest to declare.

Acknowledgement

References

[1] M. Jeguirim, B. Khiari, L. Limousy, "Biomass feedstocks", in *Char and Carbon Materials Derived from Biomass*, Elsevier, 2019, 1-38.

[2] J. Popp, S. Kovács, J. Oláh, Z. Divéki, E. Balázs, *N. Biotechnol.*, 2021, **60**, 76-84.

[3] S. S. Siwal, Q. Zhang, N. Devi, A. K. Saini, V. Saini, B. Pareek, S. Gaidukovs, V. K. Thakur, *Renew. Sustain. Energy Rev.*, 2021, **150**, article no. 111483.

[4] B. Khiari, I. Ghouma, A. I. Ferjani, A. A. Azzaz, S. Jellali, L. Limousy, M. Jeguirim, *Fuel*, 2020, **262**, 116654-116665.

[5] M. Raza, B. Abu-Jdayil, A. H. Al-Marzouqi, A. Inayat, *Renew. Energy*, 2022, **183**, 67-77.

[6] N. Zouaoui, J. F. Brilhac, F. Mechati, M. Jeguirim, B. Djellouli, P. Gilot, *J. Therm. Anal. Calorim.*, 2010, **102**, 837-849.

[7] A. A. Azzaz, M. Jeguirim, V. Kinigopoulou, C. Doulgeris, M.-L. Goddard, S. Jellali, C. Matei Ghimbeu, *Sci. Total Environ.*, 2020, **733**, article no. 139314.

[8] B. Khiari, M. Jeguirim, "Tunisian agro-food wastes recovery by pyrolysis: thermogravimetric analysis and kinetic study", in *2019 10th Int. Renew. Energy Congr. (IREC)*, IEEE, Hammamet, Tunisia, 2019.

[9] B. Khiari, M. Massoudi, M. Jeguirim, *Environ. Sci. Pollut. Res.*, 2019, **26**, 35435-35444.

[10] M. Belhachemi, B. Khiari, M. Jeguirim, A. Sepúlveda-Escribano, "Char and Carbon Materials Derived from Biomass" (M. Jeguirim, L. Limousy, eds.), Elsevier, Amsterdam, Netherlands, 2019, 69-108.

[11] L. Gašparovič, Z. Koreňová, Ľ. Jelemenský, *Chem. Pap.*, 2010, **64**, 174-181.

[12] M. G. Grønli, G. Várhegyi, C. Di Blasi, *Ind. Eng. Chem. Res.*, 2002, **41**, 4201-4208.

[13] K. Slopiecka, P. Bartocci, F. Fantozzi, *Appl. Energy*, 2012, **97**, 491-497.

[14] A. Aboulkas, *J. Therm. Anal. Calorim.*, 2016, **123**, 1657-1666.

[15] A. Tabal, A. Barakat, A. Aboulkas, K. El harfi, *Fuel*, 2021, **283**, article no. 119253.

[16] M. Jeguirim, J. Bikai, Y. Elmay, L. Limousy, E. Njeugna, *Energy Sustain. Dev.*, 2014, **23**, 188-193.

[17] I. Díaz, M. Rodríguez, C. Arnaiz, G. San Miguel, M. Domínguez, "Biomass pyrolysis kinetics through thermogravimetric analysis", in *23 European Symposium on Computer Aided Process Engineering* (A. Kraslawski, I. Turunen, eds.), Computer Aided Chemical Engineering, vol. 32, Elsevier, Amsterdam, Netherlands, 2013, 1-6.

[18] M. Jeguirim, Y. Elmay, L. Limousy, M. Lajili, R. Said, *Environ. Prog. Sustain. Energy*, 2014, **33**, 1452-1458.

[19] E. A. N. Marks, V. Kinigopoulou, H. Akrout, A. A. Azzaz, C. Doulgeris, S. Jellali, C. Rad, P. Sánchez Zulueta, E. Tziritis, L. El-Bassi, C. Matei Ghimbeu, M. Jeguirim, *Sustainability*, 2020, **12**, 6081-6096.

[20] A. Chouchene, M. Jeguirim, B. Khiari, G. Trouvé, F. Zagrouba, *J. Anal. Appl. Pyrolysis*, 2010, **87**, 168-174.

[21] A. Agrifoglio, A. Fichera, A. Gagliano, R. Volpe, *C. R. Chim.*, 2021, **24**, 1-17.

[22] A. Gagliano, F. Nocera, F. Patania, M. Bruno, D. G. Castaldo, *C. R. Chim.*, 2016, **19**, 441-449.

[23] M. Bargaoui, S. Jellali, A. A. Azzaz, M. Jeguirim, H. Akrout, *Environ. Sci. Pollut. Res.*, 2021, **28**, 24470-24485.

[24] K. Haddad, M. Jeguirim, S. Jellali, N. Thevenin, L. Ruidavets, L. Limousy, *Sci. Total Environ.*, 2021, **752**, article no. 141713.

[25] K. Mahmoudi, N. Hamdi, M. Ben Ali, S. Jellali, E. Srasra, *C. R. Chim.*, 2021, **23**, 689-704.

[26] L. Limousy, I. Ghouma, A. Ouederni, M. Jeguirim, *Environ. Sci. Pollut. Res.*, 2017, **24**, 9993-10004.

[27] S. Jellali, E. Diamantopoulos, K. Haddad, M. Anane, W. Durner, A. Mlayah, *J. Environ. Manage.*, 2016, **180**, 439-449.

[28] B. Khiari, A. Ibn Ferjani, A. A. Azzaz, S. Jellali, L. Limousy, M. Jeguirim, *Biomass Convers. Biorefinery*, 2021, **11**, 325-337.

[29] B. Khiari, M. Jeguirim, L. Limousy, S. Bennici, *Renew. Sustain. Energy Rev.*, 2019, **108**, 253-273.

[30] S. Kordoghli, B. Khiari, M. Paraschiv, F. Zagrouba, M. Tazerout, *Int. J. Hydrogen Energy*, 2019, **44**, 11289-11302.

[31] A. Chouchene, M. Jeguirim, B. Khiari, F. Zagrouba, G. Trouvé, *Resour. Conserv. Recycl.*, 2010, **54**, 271-277.

[32] S. Ali, S. A. Hussain, M. Z. Mohd. Tohir, A. A. Nuruddin, *Mater. Today Proc.*, 2021, **42**, 178-185.

[33] P. Weerachanchai, C. Tangsathitkulchai, M. Tangsathitkulchai, *Suranaree J. Sci. Technol.*, 2011, **17**, 387-400.

[34] M. Jeguirim, S. Dorge, A. Loth, G. Trouvé, *Int. J. Green Energy*, 2010, **7**, 164-173.

[35] M. Pala, I. C. Kantarli, H. B. Buyukisik, J. Yanik, *Bioresour. Technol.*, 2014, **161**, 255-262.

[36] D.-I. Kim, Y. Matsuyama, S. Nagasoe, M. Yamaguchi, Y. Ho, Y. Oshima, N. Imada, T. Honjo, *J. Plankton Res.*, 2004, **26**, 61-66.

[37] N. Grioui, K. Halouani, A. Zoulalian, F. Elhalouani, *Thermochim. Acta*, 2005, 23-30.

[38] X. Hu, M. Gholizadeh, *J. Energy Chem.*, 2019, **39**, 109-143.

[39] A.-C. Johansson, L. Sandström, O. G. W. Öhrman, H. Jilvero, *J. Anal. Appl. Pyrolysis*, 2018, **134**, 102-113.

[40] S. Sri Shalini, K. Palanivelu, A. Ramachandran, V. Raghavan, *Biorefinery*, 2020, **280**.

[41] N. Boukaous, L. Abdelouahed, C. Mustapha, C. Mohabeer, A. Meniai, B. Taouk, *C. R. Chim.*, 2021, **23**, 623-634.

[42] H. Hammani, M. El Achaby, K. El Harfi, M. Mhammedi, A. Aboulkas, *C. R. Chim.*, 2020, 1-18.

[43] S. A. El-Sayed, M. E. Mostafa, *Energy Convers. Manag.*, 2014, **85**, 165-172.

[44] R. Charvet, F. Silva, L. Ruivo, L. Tarelho, A. Matos, J. Figueiredo da Silva, D. Neves, *Energies*, 2021, **14**, article no. 2537.

[45] Y.-E. Lee, D.-C. Shin, Y. Jeong, I. Kim, Y.-S. Yoo, *Energies*, 2019, **12**, article no. 4538.

[46] T. Damartzis, D. Vamvuka, S. Sfakiotakis, A. Zabaniotou, *Bioresour. Technol.*, 2011, **102**, 6230-6238.

[47] M. Boutaieb, M. Guiza, S. Román Suero, B. Ledesma, S. Nogales, A. Ouederni, *C. R. Chim.*, 2020, **23**, 607-621.

[48] A. Anca-Couce, C. Tsekos, S. Retschitzegger, F. Zimbardi, A. Funke, S. Banks, T. Kraia, P. Marques, R. Scharler, W. de Jong, N. Kienzl, *Fuel*, 2020, **276**, article no. 118002.

[49] A. A. Azzaz, B. Khiari, S. Jellali, C. M. Ghimbeu, M. Jeguirim, *Renew. Sustain. Energy Rev.*, 2020, **127**, article no. 109882.

Jemaa Mabrouki *et al.*

[50] H. Bouaik, A. Tabal, A. Barakat, K. Harfi, A. Aboulkas, *C. R. Chim.*, 2021, **24**, 1-15.

[51] S. Niksa, *Fuel*, 2020, **263**, article no. 116649.

[52] L. Reyes, L. Abdelouahed, C. Mohabeer, J.-C. Buvat, B. Taouk, *Energy Convers. Manag.*, 2021, **244**, article no. 114459.

[53] N. Toscano Miranda, I. Lopes Motta, R. Maciel Filho, M. R. Wolf Maciel, *Renew. Sustain. Energy Rev.*, 2021, **149**, article no. 111394.

[54] S. Ceylan, Y. Topçu, *Bioresour. Technol.*, 2014, **156**, 182-188.

[55] H. Yang, R. Yan, H. Chen, C. Zheng, D. H. Lee, D. T. Liang, *Energy & Fuels*, 2006, **20**, 388-393.

[56] J. J. M. Orfão, F. J. A. Antunes, J. L. Figueiredo, *Fuel*, 1999, **78**, 349-358.

[57] A. Brillard, J. F. Brilhac, *Renew. Energy*, 2020, **146**, 1498-1509.

[58] K. N. Yogalakshmi, T. Poornima Devi, P. Sivashanmugam, S. Kavitha, R. Yukesh Kannah, S. Varjani, S. AdishKumar, G. Kumar, J. Rajesh Banu, *Chemosphere*, 2022, **286**, article no. 131824.

[59] C. Pedroza-Solis, J. De la Rosa, C. Lucio-Ortiz, D. De Haro-Del Rio, D. Casamachin, T. García, G. Escamilla, E. Carrillo-Pedraza, I. López, D. Bustos, D. Garcia-Gutierrez, L. Sandoval-Rangel, *C. R. Chim.*, 2021, **24**, 1-17.

[60] L. Luo, X. Guo, Z. Zhang, M. Chai, M. M. Rahman, X. Zhang, J. Cai, *Energy & Fuels*, 2020, **34**, 4874-4881.

[61] D. K. Ojha, D. Viju, R. Vinu, *Energy Convers. Manag. X.*, 2021, **10**, article no. 100071.

[62] P. Parthasarathy, K. S. Narayanan, L. Arockiam, *Biomass Bioenergy*, 2013, **58**, 58-66.

[63] M. V. Gil, D. Casal, C. Pevida, J. J. Pis, F. Rubiera, *Bioresour. Technol.*, 2010, **101**, 5601-5608.